

# Angular and polarization dependence of all optical diode in one-dimensional photonic crystal

Kazem Jamshidi-Ghaleh<sup>1,2,a</sup>, Zeinab Safari<sup>3</sup>, and Fatemeh Moslemi<sup>1</sup>

<sup>1</sup> Department of Physics, Azarbaijan Shahid Madani University, Tabriz, Iran

<sup>2</sup> Research Group of Processing and communication, Azarbaijan Shahid Madani University, Tabriz, Iran

<sup>3</sup> Atomic and Molecular Group, Department of Physics, Yazd University, P.O. Box 891995-741, Yazd, Iran

Received 16 November 2014 / Received in final form 24 February 2015

Published online 2 April 2015 – © EDP Sciences, Società Italiana di Fisica, Springer-Verlag 2015

**Abstract.** The effect of the incident angle on all-optical diode (AOD) efficiency in a one-dimensional photonic crystal structure (1DPC) for TE and TM polarizations was studied. An asymmetric hybrid Fabry Perot resonator type 1DPC structure composed of linear and nonlinear materials was considered in this communication. The nonlinear transmission curves around the defect mode resonant frequency inside the photonic band gap for both TE and TM polarizations at different incident angles, from left to right (L-R) and right to left (R-L) incidences, are illustrated. Results showed that with increasing the incident angle, AOD performance efficiency increases only for TM polarization. The AOD efficiency increased to 80% for an incident angle of 60 degrees because of the dynamical shifting of the defect mode peak frequency caused by the intensity-dependency of the nonlinear layer refractive index along the  $z$ -axes. For TE polarization, the  $z$ -component of the electric field remained constant for all incident angles. The results of this study can be important in optical data communications and information analysis in all-optical integrated circuits.

## 1 Introduction

In the last two and a half decades, artificial periodic structures known as photonic crystals (PCs), first introduced by Yablonovich [1] and John [2], have attracted much attention. The photonic gap, or forbidden band gap, is a remarkable feature of a PC structure which is similar to the electronic band gap in a semiconductor. The electromagnetic field of the frequency within the band gap is evanescent. Today, photonic crystal structures are employed to control and manipulate the propagation of photons and their potential applications going to be examined [3–6]. Additionally, designing an all-optical device with the ability being controlled by an external parameter has recently attracted great attention due to its important application in fields of optical communication and information processing. Because of its special electromagnetic performance and unique ability to manipulate the propagation states of photons, the PC structure is regarded as an ideal basis for integrated photonic devices [7–11].

Incorporating nonlinearity with PC structures gives one the capability of dynamically controlling wave propagation. Inouyea and Kanemitsu [12] experimentally observed mode shifting and opened up new fields in the application of PCs in nonlinear optical devices. Optical bistability is a nonlinear process that can manipulate a photon's transportation and can be used in designing all-optical switching [13]. It can be induced by the dynamic shifting of the band edge or one of the resonant

modes [14,15] which appears in the photonic band gap of a defective periodic or disordered PC structure. The performance of optical bistability in a spatially asymmetric PC structure together with the anisotropy of the field intensity distribution inside the layers makes the structure behave as a device called AOD. It permits an electromagnetic wave to pass from one side of the structure but not from the other side and is an electronic analogue of the electric diode that passes electricity from one side only. AOD has promising applications in some areas such as integrated photonic circuits, ultrafast information processing, optical isolation and interconnection systems. Spatially nonreciprocal passive AOD are currently receiving much attention as an alternative to the conventional optical isolator, which is based on linear polarizers and a magneto-optical Faraday rotator.

In recent years, various structures have been proposed to design an AOD, including using a 1D nonlinear PC with defect [16,17], 1D nonlinear PC with a spatial graduation in the linear refractive index [18], a nonlinear asymmetric Bragg reflector [19], bistable diode action in left-handed periodic structures [20] and spatial asymmetry of the structure (e.g., Thue-Morse structure) with Kerr nonlinear dielectric materials [21,22]. An electro-tunable optical diode based on liquid-crystal heterojunctions showing nonreciprocal transmission of circularly polarized light at the photonic band gap regions has also been reported [23]. In another configuration using liquid crystals as the defect layer, linearly polarized light is used [24]. The relatively low transmission because of metal absorption and

<sup>a</sup> e-mail: k-jamshidi@azaruniv.edu

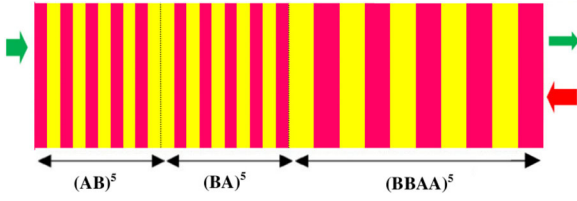


**Fig. 1.** Schematic of the 1DPC structure with the asymmetric arrangement of  $(AB)^5(BA)^5(BBAA)^5$ .

the comparatively complicated structure are among the application limitations of some proposed AODs.

As far as is known, all previous studies have been done for normal incidence, and the effects of the incident angle and state of the polarization were omitted. This work illustrates the possibility of AOD performance and its transmission contrast adjustability by incident angle and investigates the effect of polarization in an asymmetric 1DPC structure. Results of this study show that a one-way transmission property (optical diode action) from the proposed structure is achievable for the TM polarization state and sensitive to the angle of incidence but not for the TE polarization state at any incident angle.

The paper is organized as follows. In Section 2, the problem geometry is introduced and a brief description of the transfer matrix method is presented as the numerical tool in this study. In Section 3, the numerical results are presented to find the desired structures. Finally, in Section 4, the obtained results are summarized.

## 2 Theoretical model

Zhukovsky [25,26] proposed the hybrid Fabry Perot resonator 1DPC structures of the type  $(AB)^n(BA)^m(AABB)^k$  and found that it exhibited pronounced unidirectionality due to the strong spatial asymmetry of the resonant mode and high transmission caused by the existence of a perfect transmission resonance [26]. He studied the effect of periodicity numbers  $n$ ,  $m$  and  $k$  on optical bistability from this structure at normal incidence.

In this work, the hybrid Fabry Perot resonator structure of  $(AB)^5(BA)^5(AABB)^5$  was employed, where letters A and B stand for linear and nonlinear materials, respectively (see Fig. 1). The linear and nonlinear material parameters of A and B were selected as those in references [21,22,24–27], the  $\text{TiO}_2$  with  $n_A = 2.3$ ,  $n_2 \approx 10^{-8} \text{ cm}^2/\text{MW}$ , and polydiacetylene 9-BCMU organic material with  $n_B = 1.55$ ,  $n_2 = 2.5 \times 10^{-5} \text{ cm}^2/\text{MW}$ , respectively. The nonlinear response of layer A by three orders of magnitude was smaller than that of layer B; therefore, it can be neglected. It should be mentioned that the refractive index of a medium with a nonlinear response would be intensity dependent given that  $n = n_0 + n_2 I$ , where  $n_0$  is the linear refractive index,  $n_2$  the nonlinear refractive index that is related to third order susceptibility  $\chi^{(3)}$  and  $I$  is the intensity of total electric field in the medium [28]. The optical thickness of the layers was taken

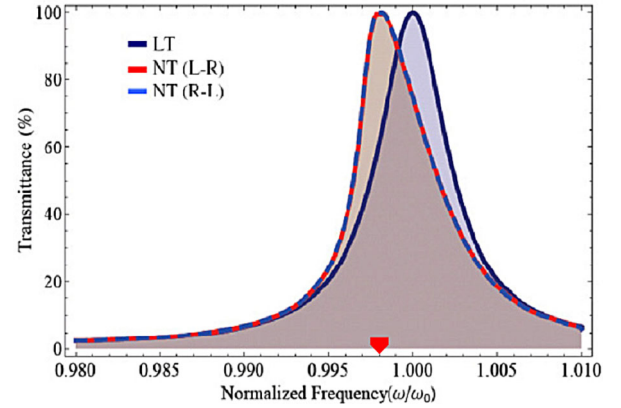


**Fig. 2.** Linear (black curve) and nonlinear transmission spectrum corresponding to L-R (blue) and R-L (red) normal propagation of light with an input intensity of  $50 \text{ MW}/\text{cm}^2$ .

to be a quarter wave:  $n_A d_A = n_B d_B = \lambda_0/4$  in which  $\lambda_0 = 550 \text{ nm}$  is the characteristic wavelength.

The well-known simple and powerful transfer matrix method for linear and nonlinear transmissions [29,30] was employed to analysis the propagation of the electromagnetic wave through the structure. According to this method, the tangential components of the electric and magnetic fields across the  $j$ th layer of width  $d_j$ , refractive index  $n_j$ , electric susceptibility  $\varepsilon_j$  and magnetic permeability  $\mu_j$  are related by the following matrix:

$$M_j = \begin{bmatrix} \cos(k_j d_j) & q_j^{-1} \sin(k_j d_j) \\ -q_j \sin(k_j d_j) & \cos(k_j d_j) \end{bmatrix}, \quad (1)$$

where

$$k_j = \frac{\omega}{c} \sqrt{\mu_j \varepsilon_j} \sqrt{1 - \sin^2 \theta / \mu_j \varepsilon_j},$$

$$q_j = \sqrt{\varepsilon_j} / \sqrt{\mu_j} \sqrt{1 - \sin^2 \theta / \mu_j \varepsilon_j},$$

for TE and

$$q_j = \sqrt{\mu_j} / \sqrt{\varepsilon_j} \sqrt{1 - \sin^2 \theta / \mu_j \varepsilon_j},$$

for TM polarization,  $\theta$  is the angle of incidence in the corresponding layer, and  $j$  stands for layers A and B. The transfer matrix for the proposed structure embedded in air can be obtained by multiplying together all transfer matrices of subsequent layer:

$$M = (M_A M_B)^5 (M_B M_A)^5 (M_A M_A M_B M_B)^5. \quad (2)$$

The transmittance in terms of the total transfer matrix elements,  $M_{ij}$ , is given by:

$$T(\omega) = \frac{4 \cos^2 \theta}{|(M_{11} + M_{22}) \cos \theta - i(M_{21} \cos^2 \theta - M_{12})|^2}. \quad (3)$$

## 3 Results and discussions

In Figure 2, the linear transmission (LT) and the nonlinear transmission (NT) spectrum from left to right (L-R) and

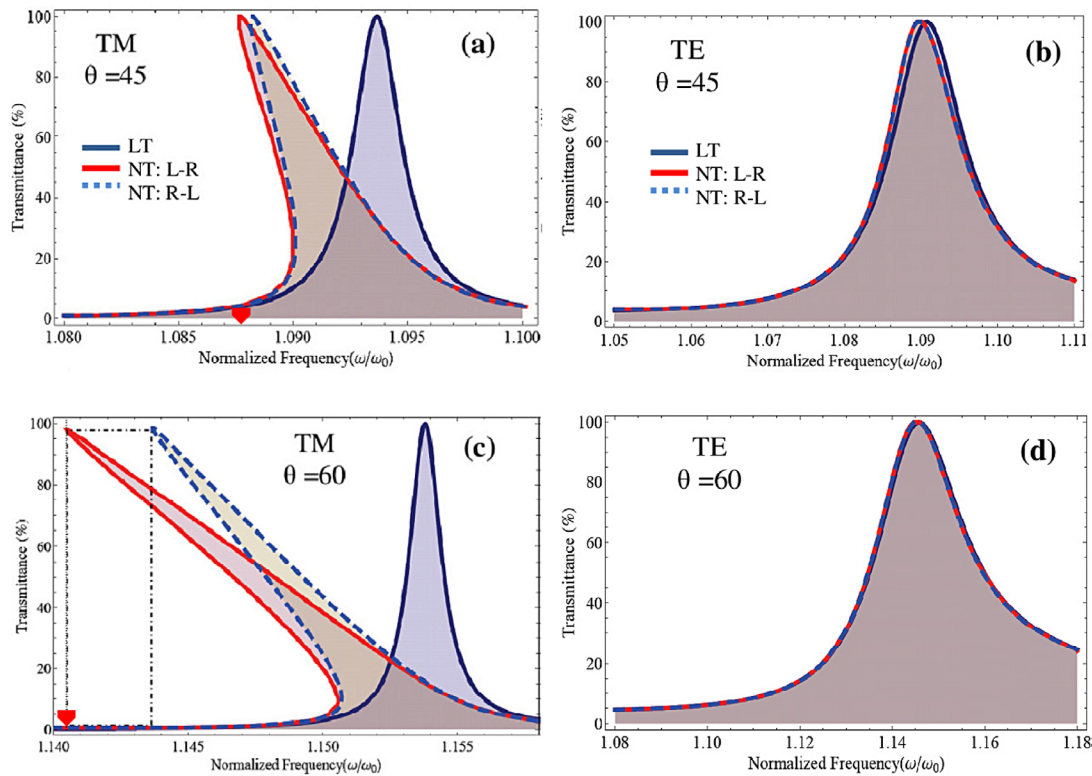


**Fig. 3.** The linear transmission (black) and behaviour of the nonlinear transmissions from L-R (dash-blue) and R-L (red) light incidence for TM and TE polarization at incident angles of 45 (a) and (b) and 60 (c) and (d) degrees, respectively. Other parameters are the same as in Figure 1.

right to left (R-L) light incidence at a normal angle is plotted. It can be seen that for both incident directions, the NT spectrums overlapped. They were also deflected to the lower frequencies with respect to the LT defect mode peak frequency. This indicates the dynamic modification of the optical path length in nonlinear layers B caused by the intensity dependence of their refractive index.

To investigate the effects of the incident angle and state of polarization, the NT spectrum for both polarization states and different angle of incidences was studied. Figure 3 shows the behaviour of the NT curves around the linear transmission peak frequency (defect mode), from L-R and R-L light incidence, for both TE and TM polarizations at incident angles of 45 and 60 degrees. It can be clearly seen that increasing the incident angle causes the NT transmission of the L-R direction to deviate faster than the R-L direction for TM polarization but it remains constant for TE polarization. The deviation of L-R and R-L transmissions in a PC structure can be used as an optical diode device. For example to estimate the AOD efficiency given by  $C = (T_{\text{Left}} - T_{\text{Right}}) / (T_{\text{Left}} + T_{\text{Right}})$  at the incident angle of 60 degrees for the TM polarization state more than 80% transmission contrast of AOD action is achievable (see dashed region in Fig. 3c). Figure 4 shows the deviation of the defect mode peak frequency for both TM and TE polarization states from L-R and R-L incidences at different incident angles. The difference between L-R and R-L transmission peak frequency increases with incident angle for TM polarization.

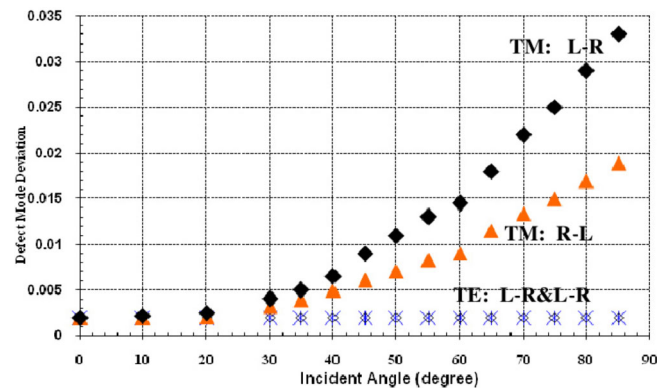


**Fig. 4.** Deviation of defect mode peak frequency for TM and TE polarizations at different incident angles.

The physical interpretation of these behaviours is very simple. One of the necessary conditions for a PC structure to display an efficient AOD performance is that the field intensity distribution inside the layers should be anisotropic for left and right side incidents. For TE polarization, the electric component of the incident field remains along the  $x$  or  $y$  direction for all incident angles and cannot affect the field distribution inside the layers (along  $z$ -axes). For TM polarization, however, the electric field is in the  $x$ - $z$  plane, and its component along the  $z$ -axis varies with varying incident angles. Then, the refractive index inside of the nonlinear

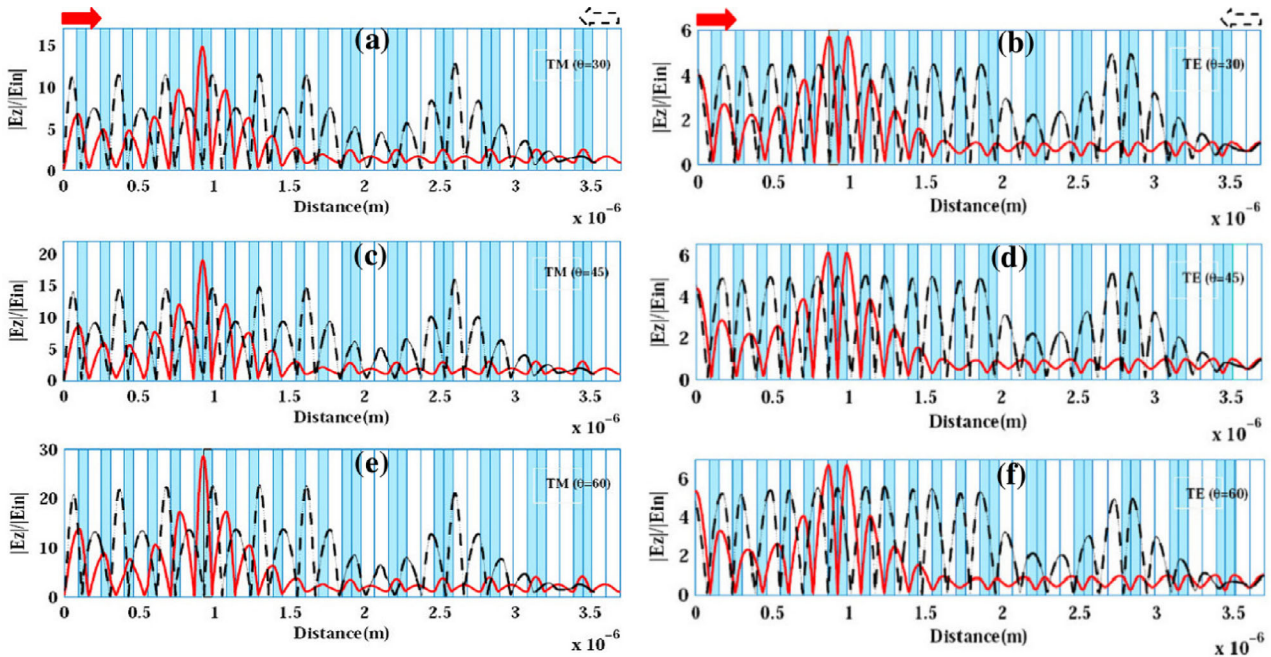


**Fig. 5.** Distribution of normalized  $z$ -components of the electric field inside layers for TM and TE polarizations, from L-R (red) and R-L (dashed) at incident angles of 30 ((a) and (b)), 45 ((c) and (d)) and 60 ((e) and (f)) degrees. It can be seen that the  $z$ -component of the electric field remains constant in all incident angles for TE polarization but increases for TM polarization.

layers will change dynamically because of its intensity dependency.

To justify those statements, the  $z$ -component of the electric field distribution (normalized to the incident field) inside the layers of the whole PC structure has been plotted for both polarizations and different incident angles as illustrated in Figure 5, from L-R (red curve) and R-L (dashed black curve). It can be seen that the electric field  $z$ -component increases with increases in the incident angle for TM polarization, but remains constant for TE polarization at all incident angles. Increasing the electric field inside the layers with nonlinear response (layers B) changes their refractive index. Accordingly, the optical path length will change. Then, the peak of the resonant mode will shift and, correspondingly, the nonlinear transmission that depends on transmission frequency will also change.

According to the above statements, the intensity of the incident light is one of the important parameters that can affect the nonlinear transmittance through the structure. In Figure 6, we have plotted the example nonlinear curves at incident angles of 0, 45 and 60 degree, around the frequencies depicted in Figures 2, 3a and 3c. The hysteresis behaviour (optical bistability) clearly visible on an output versus input intensity diagram.

### 4 Conclusion

In summary, the incident light polarization and angle effects on AOD behavior and its efficiency from a 1DPC structure with arrangement of  $(AB)^5(BA)^5(AABB)^5$ ,

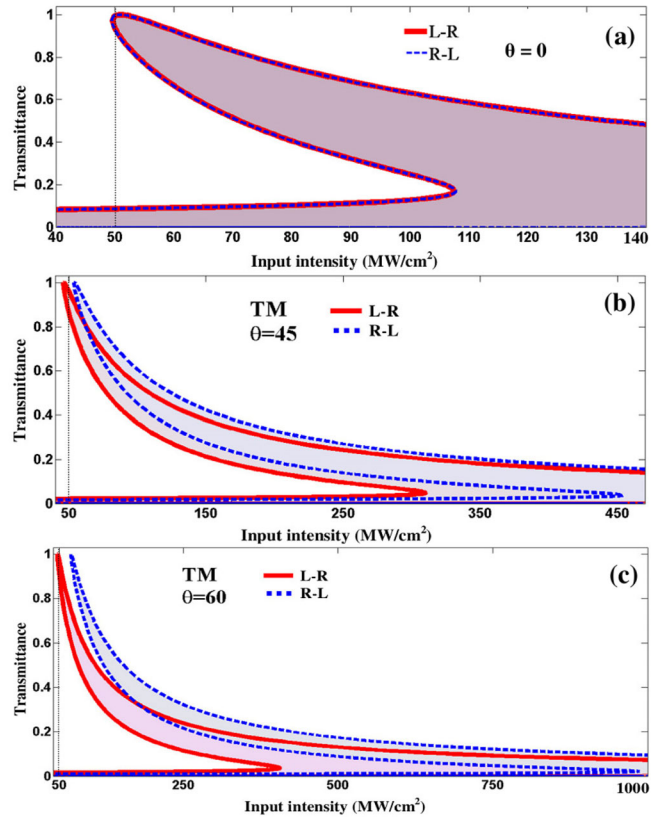


**Fig. 6.** Behaviour of nonlinear transmissions from L-R (dash-blue) and R-L (red) light incidence for normal incidence (a) and 45 (b) and 60 (c) degrees for TM polarization at different input intensities around the frequencies indicated in corresponding Figures 2, 3a and 3c.

where all layers A are linear ( $\text{TiO}_2$ ) and B nonlinear material (polydiacetylene 9-BCMU), respectively, have been illustrated. Nonlinear transmission curves around the defect mode frequency are presented for TE and TM polarization at different angle of incidences. The numerical results show that with increasing the incident angle the efficiency of AOD performance increases for the TM polarization state and reaches more than 80% on an incident angle of 60 degrees. No efficient AOD performance is observed for the TE polarization at any incident angle. This is due to the variance of the electric field component for the TM state along the PC structure period ( $z$ -axes) that dynamically affects the refractive index of the nonlinear layers. In the case of TE polarization, the electric field component remains constant for all incident angles. This may be important in optical data communications and analysis.

## References

1. E. Yablonovitch, Phys. Rev. Lett. **67**, 2295 (1991)
2. S. John, Phys. Rev. Lett. **58**, 2486 (1987)
3. I. Celanovic, F. O'Sullivan, M. Ilak, J. Kassakian, D. Perreault, Opt. Lett. **29**, 863 (2004)
4. F. O'Sullivan, I. Celanovic, N. Jovanovic, J. Kassakian, S. Akiyama, K. Wada, J. Appl. Phys. **97**, 033529 (2005)
5. R. Kakimi, M. Fujita, M. Nagai, M. Ashida, T. Nagatsuma, Nat. Photon. **8**, 657 (2014)
6. S.A. El-Naggar, Eur. Phys. J. D **67**, 54 (2013)
7. T.F. Krauss, R.M. De La Rue, Prog. Quant. Elec. **23**, 51 (1999)
8. S. Arishmar Cerqueira Jr., Rep. Prog. Phys. **73**, 024401 (2010)
9. M. Soljačić, C. Luo, J.D. Joannopoulos, S. Fan, Opt. Lett. **28**, 637 (2003)
10. S. Mingaleev, Y.S. Kivshar, J. Opt. Soc. Am. B **19**, 2241 (2002)
11. W.Y. Chiu, Y.S. Wu, Y.J. Chan, T.D. Wang, C.H. Hou, H.T. Chien, C.C. Chen, Opt. Commun. **28**, 4749 (2011)
12. H. Inouyea, Y. Kanemitsu, Appl. Phys. Lett. **82**, 1155 (2003)
13. J. He, M. Cada, IEEE J. Quantum Electron. **27**, 1182 (1991)
14. P. Tran, Opt. Lett. **21**, 1138 (1996)
15. R. Wang, J. Dong, D.Y. Xing, Phys. Rev. E **55**, 6301 (1997)
16. W. Wei-jiang, I.Z. Jin-yun, X. Wan-neng, Optoelectron. Lett. **2**, 0237 (2006)
17. M. Scalora, J.P. Dowling, C.M. Bowden, M.J. Bloemer, J. Appl. Phys. **76**, 2023 (1994)
18. M. Scalora, J.P. Dowling, C.W. Bowden, M.J. Bloemer, Phys. Rev. Lett. **73**, 1368 (1994)
19. M.D. Tocci, M.J. Bloemer, M. Scalora, J.P. Dowling, C.M. Bowden, Appl. Phys. Lett. **66**, 2324 (1995)
20. M.W. Feise, I.V. Shadrivov, Yu.S. Kivshar, Phys. Rev. E **71**, 037602 (2005)
21. F. Biancalana, J. Appl. Phys. **104**, 093113 (2008)
22. V. Grigoriev, F. Biancalana, New J. Phys. **12**, 053041 (2010)
23. J. Hwang, M.H. Song, B. Park, S. Nishimura, T. Toyooka, J.W. Wu, Y. Takanishi, K. Ishikawa, H. Takezoe, Nat. Mater. **4**, 383 (2005)
24. J.Y. Chen, L.W. Chen, Opt. Express **14**, 10733 (2006)
25. S.V. Zhukovsky, A.G. Smirnov, Phys. Rev. A **83**, 023818 (2011)
26. S.V. Zhukovsky, Phys. Rev. A **81**, 053808 (2010)
27. L. Jin, J. Zhou, M. Yang, C. Xue, M. He, Opt. Eng. **50**, 030503 (2011)
28. R.W. Boyd, *Nonlinear Optics*, 3rd edn. (Academic press, San Diego, 2008)
29. P. Yeh, *Optical Waves in Layered Media* (John Wiley & Sons, New York, 2005)
30. M. Born, E. Wolf, *Principles of Optics: Electromagnetic Theory of Propagation, Interference and Diffraction of Light* (Pergamon Press, Oxford, 1964)